On the nature of type 1 AGN: emission properties and correlations

Irham Taufik Andika[1], Mochamad Ikbal Arifyanto[1], Wolfram Kollatschny[2]

[1]Astronomy Study Program, Institut Teknologi Bandung, Jl. Ganesha No. 10, Bandung 40116, Indonesia
[2]Institut for Astrophysics, University of Goettingen, Friedrich-Hund-Platz 1, Goettingen 37077, Germany

E-mail: irham.andika@students.itb.ac.id

Abstract. We present a study of emission properties and correlations of 3191 type 1 AGN at $z < 0.35$, selected from Sloan Digital Sky Survey Data Release 12. We supplement the data with ultraviolet spectra from Hubble Space Telescope and International Ultraviolet Explorer along with X-ray properties from Chandra Source Catalog and XMM-Newton Serendipitous Source Catalog and radio measurements from FIRST. We find that the observed spectral diversity of type 1 AGN can be unified by Eddington ratio ($L/L_{\rm Edd}$). Objects with higher $L/L_{\rm Edd}$ tend to have narrower broad Hβ component, strong Fe II emission, systematic blueshift of C IV λ1549, soft X-ray excess, and lower ionization parameter compared to those of the lower $L/L_{\rm Edd}$.

1. Introduction

The term of active galactic nuclei (AGN) is related to the compact region at the center of galaxy that emits more radiation (up to several order of magnitude) than the rest of the host galaxy. The central engine of AGN are thought to be powered by accretion of gas (in the form of accretion disk) onto supermassive black hole (SMBH; [1]). This accretion disk generates energy which is then released in the form of radiation, winds, and/or jets which photoionizes the gas located near the center of AGN [2]. The region of the circumnuclear gas can be divided into two categories based on its physics and kinematics: broad line region (BLR) located closer (≤ 1 pc) to SMBH, which produces permitted emission lines with typical width thousands of km s^{-1}, and narrow line region (NLR), located further from SMBH, which produces permitted and forbidden emission lines with typical width hundreds of km s^{-1}.

In order to understand the physical mechanisms in BLR and NLR, many attempts have been made to find correlation among different observable properties of AGN. One of those interesting correlations is eigenvector 1 (EV1) correlation, originally found in the Palomar-Green (PG) quasar sample [3] and then studied further by several authors in context of 4DE1 (4 Dimensional Eigenvector 1; [4]). In term of EV1 correlation, objects that have strong Fe II emission tend to have narrow Hβ width and weak [O III] emission. Based on [1], the optical complex Fe II lines are believed to come from BLR while narrow Hβ and [O III] lines are emitted by NLR. The predominant factor that appears to be driving this correlation is Eddington ratio,

$L/L_{\rm Edd}$ [5]. The EV1 correlation is somewhat unexpected as BLR and NLR properties are physically different. NLR can be described as low-density and low-velocity gas extending from outer AGN torus up to thousands of parsecs along the general direction of ionization cones. This makes NLR emission not only driven by photoionization from accretion disk of AGN but also affected by the host galaxy. Therefore, it is important to study the connection BLR and NLR spectral properties while considering host galaxy contribution to AGN emission, especially for low luminosity AGN.

In this work, we present a new Sloan Digital Sky Survey Data Release 12 [6] based sample of selected type 1 AGN. Type 1 AGN is class of AGN which shows broad permitted and semi-forbidden emission lines and a bright, non-stellar, central point source visible at all wavelengths that are not contaminated by stellar light as the consequences of direct view to the nucleus based on AGN unification scheme [1]. Then, we supplement the data with spectral data based on Hubble Space Telescope (HST) and International Ultraviolet Explorer (IUE) archives and X-ray properties from Chandra Source Catalog [7] and XMM-Newton Serendipitous Source Catalog [8]. Using this data set, we explore the emission properties and correlation to study the nature of type 1 AGN.

Throughout this paper, we assume a Friedmann-Robertson-Walker cosmology with $\Omega = 0.3, \Lambda = 0.7, H_0 = 70$ km s^{-1} Mpc^{-1}.

2. Data

2.1. Main sample construction

We derived the data based on Sloan Digital Sky Survey (SDSS) Data Release (DR) 12 [6] in order to derive a well-defined sample of type 1 AGN at low redshift (z). We search the AGN data in SDSS DR 12 database using these criteria:

(i) The spectrum of the objects is classified as quasi-stellar object or "QSO" by SDSS pipeline.

(ii) $0.02 \leq z \leq 0.35$, to cover the Balmer series (especially Hβ and Hα), optical forbidden narrow lines [O II], [O III], [N II], [S II], and optical Fe II complex in the spectral lines.

(iii) S/N > 10 in the spectrum based on median S/N of whole pixels covered by the spectrum (available in the SDSS database), to improve the accuracy of NLR/BLR decomposition.

(iv) High confidence in redshift determination.

A total 9184 spectra pass our criteria. We name them as "main sample". The reduced one-dimensional (1D) spectral data are downloaded through the SDSS Skyserver (http://skyserver.sdss.org/dr12/en). To include soft X-ray photon index Γ_s measurement, we matched our AGN with the Chandra Source Catalog (CSC; [7]) and the XMM-Newton Serendipitous Source Catalog [8] with a matching radius of 1". The 1σ measurement uncertainties in Γ_s are typically $\sim$ 10% (relative uncertainty) for Chandra sources, and $\sim$ 20% (relative uncertainty) for XMM-Newton sources. To include radio properties, we match the main sample data with FIRST [9] catalog with a matching radius of 30". Then, we compute the integrated radio flux density at 20 cm and classify T1 AGN into radio loud or radio quiet AGN [10].

In order to derive a well-defined type 1 AGN sample, we utilize the diagnostic diagram to classify our sample [13]. Therefore, we exclude objects reside other than AGN regime in diagnostic diagram so that our sample now contains 3191 AGN. We named this sample as 'T1 AGN'. We obtained 31 UV spectral data from HST and IUE. The number of X-ray sources from CSC and XMM-Newton Serendipitous Source Catalog that matched with our T1 AGN is 38 and the number of radio source from FIRST that matched with our T1 AGN is 310. The T1 AGN reside at $42.4 < \log L_{5100} < 45.3$ with median $\log L_{5100} = 43.9$, where L_{5100} is averaged continuum luminosity at rest wavelength 5100 Å.

2.2. Spectral measurements

The data processing throughout this paper were done using custom software using *Python* (*Python* is an interpreted, interactive, object-oriented programming language). We use similar approach described by [11] with some modifications in continuum and emission lines fitting procedure. We separated the continuum windows into three parts: around [O II], Hβ, and Hα. For each region, we fit a local power-law continuum ($f_\lambda = A\lambda^{\alpha_\lambda}$), an iron template, and host galaxy spectra to the wavelength region around the line that is not contaminated by the emission line.

We compare our results with the $L_{[\mathrm{O\ III}]}$ measurements of SDSS AGN in [12], who model [O III] using multiple Gauss-Hermite (GH) functions. In the 2657 overlapping objects, the mean difference of our $L_{[\mathrm{O\ III}]}$ to Stern & Laor $L_{[\mathrm{O\ III}]}$ is 0.1 dex with dispersion of 0.08 dex. A total of 4293 objects with acceptable fits (reduced $\chi^2 < 2$) pass these criteria. We note that our rejection criteria may have been too restrictive, and potentially excluded objects with an unusual broad line profile.

3. Result and analysis

3.1. T1 AGN distribution in 4DE1 plane

The original optical plane of 4DE1 involved measures of FWHM bHβ and the $R_{\mathrm{Fe\ II}}$ [4]. The $R_{\mathrm{Fe\ II}}$ represents the ratio between equivalent width of Fe II within $4434 - 4684$ Å to equivalent width of broad Hβ. The $R_{\mathrm{Fe\ II}}$ proposed by [4] only consider $\sim 25\%$ Fe II strength in optical region. Here we modify $R_{\mathrm{Fe\ II}}$ into $L_{\mathrm{Fe\ II}}/L_{\mathrm{bH}\beta}$ because physically $L_{\mathrm{Fe\ II}}/L_{\mathrm{bH}\beta} \propto R_{\mathrm{Fe\ II}}$. We also account $L_{\mathrm{Fe\ II}}$ in the wider range, i.e. $4000 - 5500$ Å, to account $\sim 100\%$ Fe II strength in optical region. The $L_{\mathrm{Fe\ II}}/L_{\mathrm{bH}\beta}$ can be interpreted as physical condition of the emitting gas (density, ionization, and metallicity) while FWHM bHβ is widely used as a virial estimator. Higher $L_{\mathrm{Fe\ II}}/L_{\mathrm{bH}\beta}$ means higher ionization degree and metallicity in BLR gas while higher FWHM bHβ usually caused by higher center SMBH mass and vice versa [1].

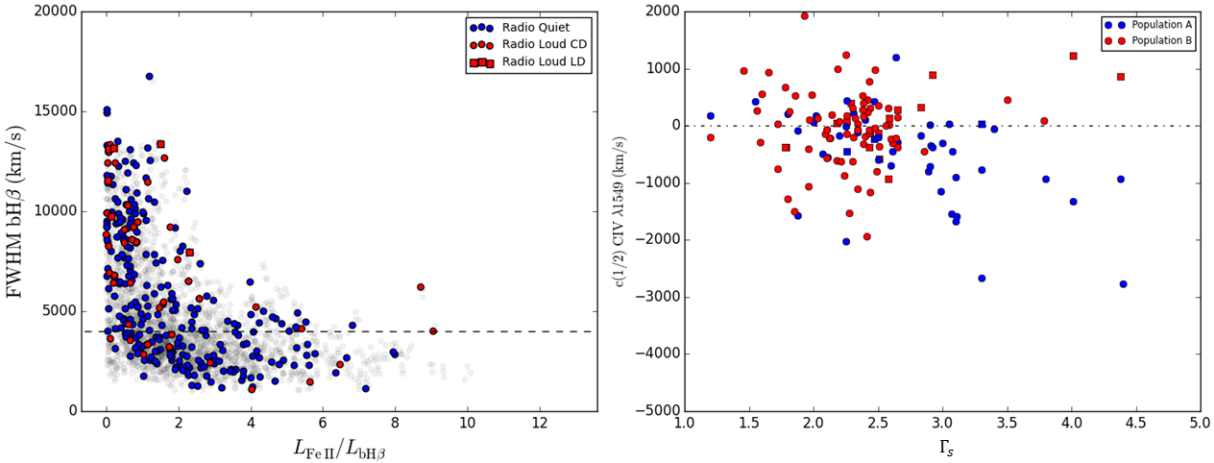

Figure 1. Left panel: T1 AGN in the 4DE1 optical plane. The blue dots represent the radio-quiet objects while the red dots are the radio-loud objects. Object without radio flux measurement available are marked with gray dots. Right panel: T1 AGN in the 4DE1 UV X-ray plane. The objects with dot symbol were taken from [15] while objects with square symbol were measured in this work.

The distribution of T1 AGN in 4DE1 optical plane shown in figure 1. We divide the T1 AGN into two populations with the boundary of separation at 4000 km s^{-1}. We adopt this as

tentative boundary between population A and B as previously suggested by [4]. From the figure 1, it is clear that AGN with strong Fe II tend to have narrower Hβ. In terms of optical spectra, we can see there is no difference between radio loud and radio quiet objects because those two population distribution overlap each other in 4DE1 optical plane.

In the context of 4DE1, we can describe population A sources as showing narrower broad Hβ component, moderate or strong Fe II emission, a systematic blueshift or asymmetry of high ionization lines (in this case C IV λ1549) and a soft X-ray excess. On the other hand, population B shows broader broad Hβ component, weak Fe II emission, and almost absence of a C IV blueshift or soft X-ray excess. Figure 1 shows a correlation between soft X-ray excess (Γ_s) and the centroid shift of C IV (c(1/2)). A soft X-ray excess occurs in sources with the largest C IV blue shift which means population A often have larger soft X-ray excess than population B.

4. Conclusion

In this paper, we derive a well-selected sample of type 1 AGN at low redshift using large sample SDSS DR 12 data to get the optical spectra of the sample. Then, this data set combined with UV spectral properties from HST and IUE, along with X-ray properties from CSC and XMM-Newton SSC. Spectral reduction and analysis to optical and UV spectra carried out in order to derive emission lines parameters. We use the measured emission lines parameters to explore correlation and properties of type 1 AGN emission.

The collective evidence from T1 sample spectral properties in context of 4DE1 leads to simple interpretation. There is no significant difference in optical emission lines properties between radio loud and radio quiet AGN. By dividing T1 sample into two population based on FWHM bHβ, we found population A (FWHM bHβ < 4000 km s^{-1}) have narrower broad Hβ component, moderate or strong Fe II emission, a systematic blueshift or asymmetry of C IV λ1549 and soft X-ray excess. On the other hand, population B shows broader broad Hβ component, weak Fe II emission, and almost absence of C IV λ1549 blueshift or soft X-ray excess.

Acknowledgments

We thank Jelena Kovačević and Jonathan Stern for providing us the iron template and host galaxy eigenspectra. Also thanks to Jack Sulentic and Paola Marziani for help and useful discussion. ITA acknowledge the award of Erasmus Mundus Action 2, which supported the funding to stay at University of Goettingen, where much of this work was completed.

References

[1] Netzer H 2013 *The Physics and Evolution of Active Galactic Nuclei*
[2] Osterbrock D E, Ferland G J 2006 *Astrophysics of gaseous nebulae and active galactic nuclei*
[3] Boroson T A, Green R F 1992 *ApJS* **80** 109
[4] Sulentic J W, Zwitter T, Marziani P, Dultzin-Hacyan D 2000 *ApJ* **536** L5
[5] Boroson T A 2002 *ApJ* **565** 78
[6] Alam S *et al* 2015 *ApJS* **219** 12
[7] Evans I N *et al* 2010 *ApJS* **189** 37
[8] Watson M G *et al* 2009 *A&A* **493** 339
[9] White R L, Becker R H, Helfand D J, Gregg M D 1997 *ApJ* **475** 479
[10] Sulentic J W, Zamfir S, Marziani P, Dultzin D 2008 *in Revista Mexicana de Astronomia y Astrofisica Conference Series* 5158 (arXiv:0709.2499)
[11] Shen Y *et al* 2011 *ApJS* **194** 45
[12] Stern J and Laor A 2012 *MNRAS* **426** 2703
[13] Kewley L J, Dopita M A, Sutherland R S, Heisler C A, Trevena J 2001 *ApJ* **556** 121
[14] Shen Y, Ho L C 2014 **Nature 513** 210
[15] Sulentic J W, Bachev R, Marziani P, Negrete C A, Dultzin D 2007 *ApJ* **666** 757